Initial tests on reversed open filters on sand-covered rock mounds

van de Ven, Daan; Hofland, Bas; van Kester, Dennis; Smith, Greg; Antonini, Alessandro

Publication date
2023

Document Version
Final published version

Published in
Procedings ICE Breakwaters conference 25-27 April 2023

INITIAL TESTS ON REVERSED OPEN FILTERS ON SAND-COVERED ROCK MOUNDS

Daan van de Ven[1,2], Bas Hofland[1], Dennis Van Kester[2], Greg Smith[2], Alessandro Antonini[1]*

[1]Delft University of Technology, Netherlands
[2]Van Oord, Netherlands
** Corresponding author, email: b.hofland@tudelft.nl*

ABSTRACT

When constructing land reclamations, often sand is placed on top of the coarse rock of the bund surrounding the reclamation. The use of a geometrically open filter between the interface of sand and rock could be cost effective. It is expected that even a geometrically open filter with sand on top of gravel might be stable due to the arching mechanism. For such a "reversed" open filter the actual stability is unknown. Hence this study focusses on the stability of a reversed geometrically open filter under cyclic loading. This paper mainly describes the development of the test setup. First the numerical model OpenFOAM was used to extract the gradients from a representative case study. Next a test setup was developed to generate these low-magnitude loads at full-scale. Various sand-filter combinations were tested, with a range of ratios of the diameters of the gravel filter (D_{15F}) and the sandy base layer (D_{85B}) and sand with a unimodal distribution. They were tested for both parallel ($i_{//}$) and perpendicular ($i_{\perp}$) gradients. The order of magnitude of the occurring gradients obtained with the numerical model for the case-study were a parallel gradient of $i_{//,2\%} \approx 1\%$, decreasing to 0 going downward, and a rather constant perpendicular gradient of $i_{\perp,2\%} = 0.2\text{-}0.3$ for the lowest 4 m of the reversed granular filter. The critical perpendicular gradients were estimated at $i_{\perp c} \approx 0.2$ to 0.1 for filter ratios of $D_{85F}/D_{15B} = 7.5$ to 9.5. The critical parallel gradients were measured at $i_{//c} \approx 2\%$ down to 1%, but might be influenced by simultaneously occurring perpendicular gradients. Even though for the test case no stable situation could be proven with respect to the perpendicular gradient, realistic situations with stable reversed open filters seem possible.

1. Introduction

When constructing land reclamations, often sand is placed on top of the coarse rock of the bund surrounding the reclamation. An example cross section is given in Figure 1.

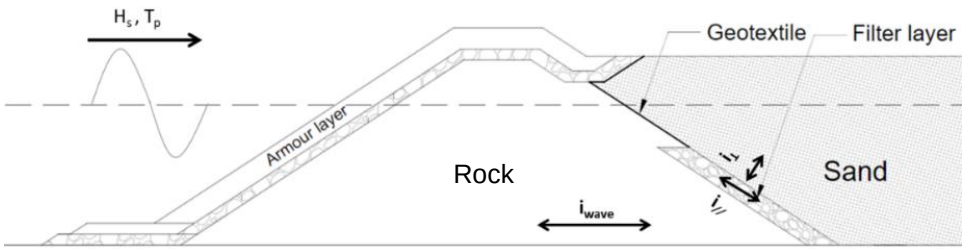

Figure 1. Example of a rock bund section with reverse open filter. Wave parameters in plot are significant wave height H_s and peak period T_p.

Making a geometrically closed filter between the bund and the sand can be laborious. Hence the use of a geometrically open granular filter could be cost effective. For such a 'reversed' open filter the hydraulic attack was studied by Polidoro et al. (2015), but the actual stability of such an open filter is unknown. Hence this study is focussed on the stability of a reversed geometrically open filter under cyclic loading. This paper mainly describes the development of the test setup. First the numerical model OpenFOAM was used to illustrate the occurring hydraulic gradients from a representative case study. This case-study is described in Section 2. Section 3 describes a test setup that was developed to generate these low-magnitude loads at full-scale. Various sand-filter combinations were tested, with a range of ratios of the diameters of the gravel filter (D_{15F}) and the sand base layer (D_{85B}). They were tested for both parallel ($i_{//}$) and perpendicular ($i_\perp$) gradients. The first results for critical gradients as derived from the results are presented in Sections 4. Sections 5 and 6 discuss the results and give conclusions.

1.1 Basic processes

Formal closed filter rules dictate that the larger grains in the sand (D_{85B}), should not fit through the pores of the filter, the size of which is dictated by the smaller grains of the filter (D_{15F}). The maximum ratio of these diameters is roughly $D_{85B}/D_{15F} < 5$. An open filter is characterized by a larger ratio of these diameters. In a normal open filter, with sand underneath the filter, the base material is stabilized by gravity, and it is regarded as being stable if the hydraulic load is below a critical threshold. The load is characterized by the two components of the hydraulic gradient on the interface, $i = \mathrm{d}p/\mathrm{d}x \,/\, \rho g$ where p is pressure relative to hydrostatic pressure, x a spatial coordinate, ρ density, and g gravitational acceleration. The parallel gradient $i_{//}$ drives the larger flow velocity inside the coarse filter layer. The perpendicular gradient $i_\perp$ drives the flow inside the sand layer. The left plot of Figure 2 illustrates these two gradient components.

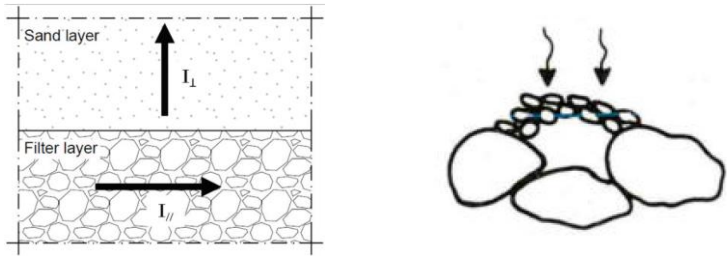

Figure 2. Left: the two hydraulic gradients acting at the interface, each determined in another medium. Right: Arching mechanism stopping sand transport through larger filter pore (De Graauw, 1983, plotted upside-down).

Because for a reversed filter gravity does not stabilize the base material, a stable filter would not seem to be possible. However, the arching effect, that influences the stability of the interface for normal filters also might occur here. Arching is the interlocking of particles that form a pressurized arch over a gap that prevents other particles to pass, as illustrated in the rights plot in Figure 2. Arching has been shown by several studies for various applications (De Graauw, 1983; Chew et al. 2003; Chen et al., 2011, Low et al., 1995; Paik and Salgado, 2003; Enstad, 1975). De Graauw (1983) states for a normal open filter that particularly the critical perpendicular gradient increases with an increased superimposed load on the material on the interface.

2. Numerical modelling to estimate load

2.1 Setup

As a test case to illustrate what gradients occur on an interface of a realistic structure, these gradients were determined by the numerical model OpenFOAM (Jacobsen et al. 2012). The use of OpenFOAM for the determination of hydraulic gradients inside rubble mounds has been validated by Jacobsen et al. (2015). For the present study no separate validation was performed. A slight deviation of the occurring values is allowed, as the study is intended to see whether in terms of order of magnitude the solution might be feasible.

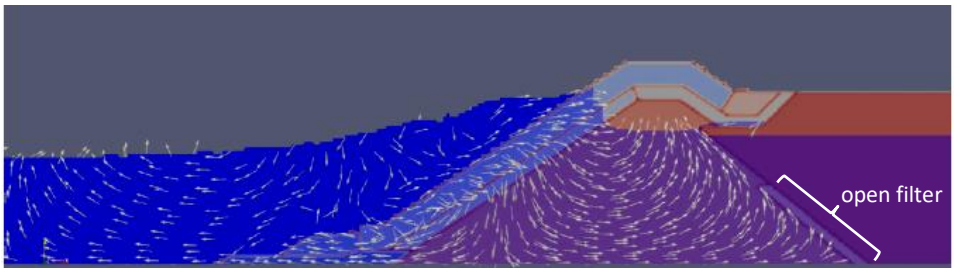

Figure 3. Part of the numerical wave flume used to estimate the gradients at the interface of a reversed open filter.

A structure as shown in Figure 1 was modelled in OpenFOAM (1.5-dev revision 1740). The modelled structure with vectors indicating the flow direction is shown in Figure 3. The water domain was larger than shown, about 1.5 wave lengths L_{op}. The applied parameters for the granular layers are given Table 1. Note that the sand fill was also permeable, be it much less than the rock bund.

Table 1. Applied coefficients for porous materials in OpenFOAM model.

Layer	porosity	D_{n50} (mm)
Core	0.4	220
Granular filter	0.4	15
Sand fill	0.36	0.1

The modelled wave climate in the OpenFOAM model is an irregular JONSWAP spectrum with target conditions of H_s = 3.5 m and T_p = 11 s. The water depth h is 12.4 m. The duration of a single simulation is 250 s. These are prototype values. The highest wave with a height of H_{max} = 5.1 m enters the domain at t =188 s. The largest wave can roughly be expected to have the exceedance value of 1/25 = 4% of the waves. However, the value of H_{max}/H_s is very close to that of a 2% exceedance value according to the Rayleigh distribution. Hence this maximum recorded wave height is taken to represent the $H_{2\%}$, the wave height exceeded by 2% of the waves. The maximum gradients were caused by this largest wave from the record. These were taken to describe the extreme loads on the interface with a 2% exceedance probability per wave, indicated by so $i_{//,2\%}$ and $i_{\perp,2\%}$.

2.1 Results

In Figure 4 the temporal behaviour of the parallel and perpendicular gradients halfway the of the open filter are shown. The right graphs indicate the location in resp. the filter and sand layer where the gradients were determined. The gradients follow the sinusoidal

motion imposed by the waves interacting with the structure, with the same 25 single waves.

Note that the perpendicular gradient halfway the filter gets a positive offset from around t = 200 s, the time that the largest waves hits the structure. This positive value indicates an upward flow, hence a downward pressure gradient. Due to this offset, even the largest troughs of the remaining waves in the signal hardly go below 0. This is caused by an internal setup of water in the rock core, that imposes a flow into the sand layer. This effect of internal setup was previously modelled by e.g. Jacobsen et al. (2015). Note that with a falling water level, also a negative offset could occur.

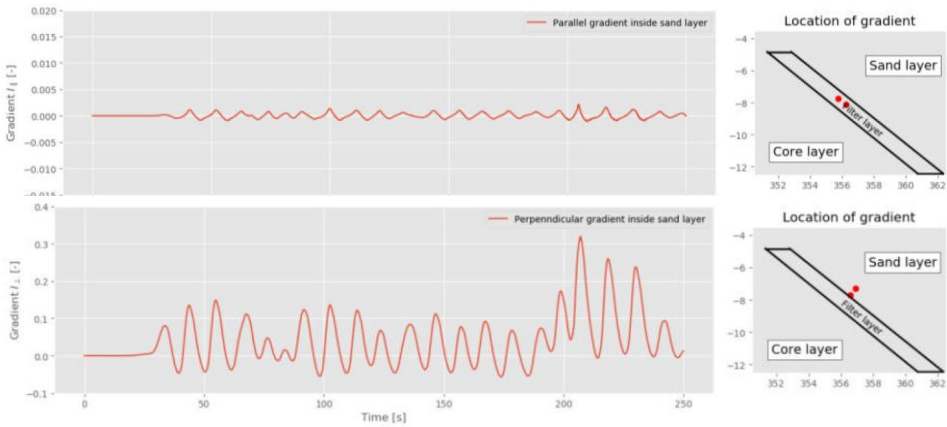

Figure 4. Simulated parallel (top) and perpendicular (bottom) hydraulic gradients as function of time halfway the filter layer at 8 m below the water surface.

Figure 5 shows the maximum (absolute) gradients at the open filter layer over the depth, so lower than 5 m below the mean water level. Whereas the order of magnitude of the parallel gradients is 1% to 2%, the order of magnitude of the perpendicular gradients is 20% to 50%. Polidoro et al. (2017) reported measured parallel gradients of the same order (1% to 3%, with exceptions up to 5%), but did not report perpendicular gradients. Both gradient components decrease going downward towards the bed. However, where the parallel gradients tend to zero near the bed, the perpendicular gradients remain constant at a value around $i_{\perp,2\%} \approx 0.25$ to 0.3.

An estimate of the perpendicular gradient can be made by dividing an estimate of the pressure at the interface, e.g. the maximum wave amplitude ($H_{max}/2$), by the height of saturated sand layer above the interface (vertical coordinate z). This crude estimate of the perpendicular gradient near the bed gives the right order of magnitude of the perpendicular gradient.

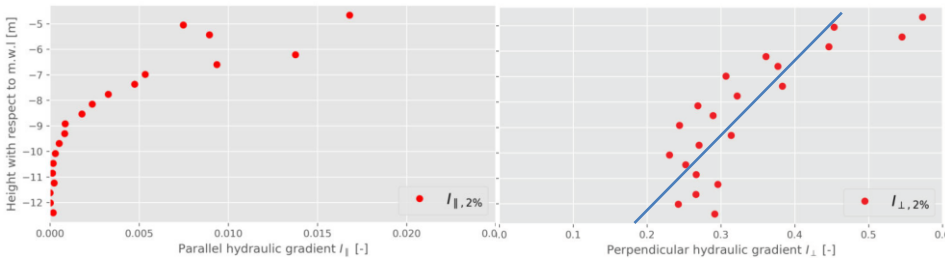

Figure 5. Calculated gradients along the lower part of the sand gravel interface vs. elevation. Left: $i_{//,2\%}$, right: $i_{\perp,2\%}$. Note the different scales of the horizontal axes. Blue line: crude estimate of perpendicular gradient, $i_{\perp} \approx H_{max}/2z$, where z is elevation relative to water level.

3. Physical modelling to estimate strength

3.1 Test setup

In order to measure the critical gradients for a reversed filter, a model setup was developed. After five iterations a suitable setup was found (Van de Ven 2018). The main parameters that play an important role in the interface stability are the forcing, given by hydraulic gradient ($i_{\parallel}$ and $i_{\perp}$), and the strength, given by the grain size ratio between granular filter and base layer D_{15F}/D_{85B}. These aspects were represented in the setup. A third factor, the superimposed load, was not varied elaborately at present.

The critical gradient was tested in a small tank of 1.00 m long, 0.15 m wide and 0.45 m high. The tank was divided in three compartments, see Figure 6. The side compartments were used to drive the flow, with a plunger forcing the water motion in one of these compartments. The 52 cm wide middle compartment contained the layers of sand and gravel (10 cm thickness), of which the interface stability was tested. Below these layers six empty compartments were situated that carried the gravel layer, and where the eroded sand could be observed. The sides of the sand layer were closed off by plywood. The sides and bottom of the gravel layer were closed off with wire mesh. This mesh was much more permeable to water than the gravel, but held the gravel in place. Between gravel and Perspex sidewalls bubble wrap was installed, that still allows visual inspection, but prevents too large flow velocities in the area with lower gravel porosity at the side walls. The plunger, with horizontal dimensions 0.22 m by 0.14 m, was connected to a strong stepper motor.

The setup was installed in a different manner for the perpendicular and parallel gradients. This can be seen in the right plots of Figure 6. For the two flow/gradient components, the setup was utilized in different modes. In order to measure the parallel gradient the top of the middle section was closed off, such that a pure parallel flow was forces along the interface. In this mode a geotextile was attached to the plywood sides of the middle section

and extended ca. 5 cm along the interface, such that no sand leakage could occur at the edges. The perpendicular gradient was modelled by closing off one side of the middle compartment and opening the top of the (now somewhat thicker) sand layer, such that the flow was forced through the sand layer.

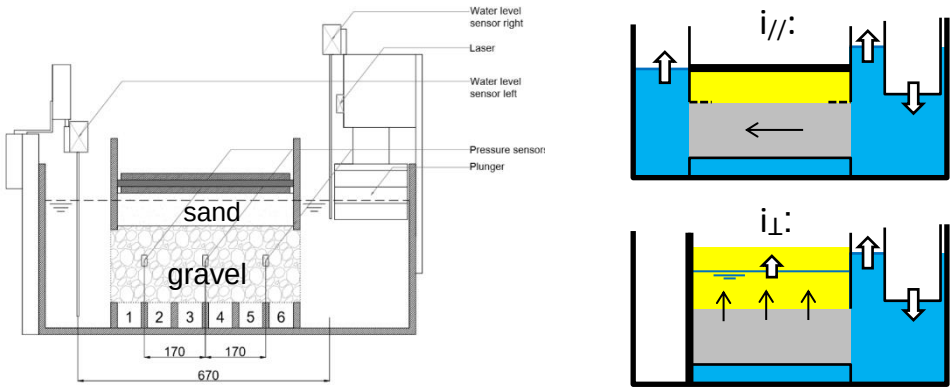

Figure 6. Left: test setup for testing interface stability. Right: indication of modes of application for parallel (top) and positive perpendicular (bottom) gradient of filter velocity.

Three different types of sand, and two types of gravel were used to obtain various filter ratios, D_{15F}/D_{85B}. The gradings of the sand and filter materials are given in Figure 7. Before every test series with a new filter setup, the entire setup was cleaned. Sand was removed from the granular filter material. Next the granular filter and pressure sensors were installed and the water level was increased to the top of the gravel layer. Then the sand was installed in the dry. Afterwards, the water level was slowly increased up to a depth of 35 cm from the tank bottom.

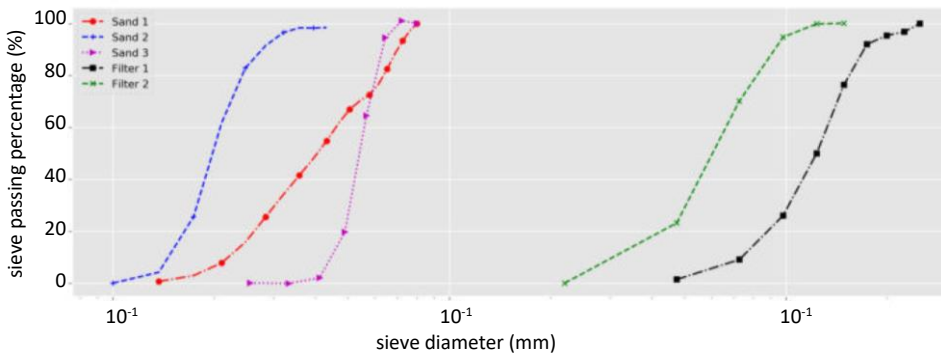

Figure 7. Grading curves of applied materials.

3.2 Measurements

Visual / video observation of sand motion. Of the six compartments underneath the gravel section, the middle four boxes were used to distinguish the initial motion of sand, to discard possible disturbances at the sides. A webcam was placed in front of the setup that recorded an image every 30 s. The test could thereby be monitored remotely. This resulted in a 4 minute movie of an entire 48 hour test sequence.

Pressure sensors. Two or three pressure sensors (*Honeywell 24PCE*, vented gauge, 34 mbar range) were applied inside resp. the sand or filter layer for resp. the perpendicular and parallel gradients. The sensors were glued in 5 cm long small tubes to enable a watertight connection with the cable. Before installation the air was removed from the 3 mm hole connecting the membrane to the water. The 20 Hz signal was low-pass filtered at 1 Hz to remove high frequency noise. The parallel gradient was measured by three pressure sensors in the middle of the gravel layer, spaced 200 mm apart. The outer two sensors with a 400 mm spacing were used for the final processing. The perpendicular gradient was measured by two pressure sensors in the middle of the sand layer, spaced 40 mm apart.

Water levels in the two compartments were measured by resistive type wave gauges (Deltares). The *plunger motion* was measured by a laser distance sensor (*optoNCDT 1302*).

3.3 Test program

The typical settings for the test sequence for all filter setups was developed in 6 repeated iterations with the filter of test Perp8.0 (see Table 2). This resulted in the following test sequence.

The initial part of a test consisted of a preliminary 2 hr ‘shakedown’ test with low gradients, as trial reference tests had shown that the model strength against erosion increases over time right after placement. After that, the real test sequence was run. In one test, consecutive periods with increasing ‘orbital’ plunger velocity (and constant plunger stroke) were run. The test signal consisted of alternating constant ‘orbital’ plunger velocities and constant plunger stroke. Each constant ‘orbital’ velocity was run for three hours. The total test typically was set to simulate about 16 different gradients, thus had a duration of up to 48 hours. In Table 2 the tests that were performed are listed.

Table 2. Applied test programme.

Test ID	D_{15F}/D_{85B}	tested range	step Δi
Par4.0	4.0	$i_{//} \approx 0.05 – 0.1$	≈ 0.002
Perp4.0		$i_{\perp} \approx 0.5 – 1.0$	≈ 0.02
Par7.5	7.5	$i_{//} \approx 0.005 – 0.05$	≈ 0.002
Perp7.5		$i_{\perp} \approx 0.1 – 0.5$	≈ 0.02
Par8.0	8.5	$i_{//} \approx 0.0025 – 0.05$	≈ 0.003
Perp8.0		$i_{\perp} \approx 0.05 – 0.5$	≈ 0.01
Par9.5	9.5	$i_{//} \approx 0.0025 – 0.05$	≈ 0.001
Perp9.5		$i_{\perp} \approx 0.05 – 0.5$	≈ 0.01
Par16.5	16.5	$i_{//} \approx 0.0025 – 0.005$	≈ 0.001
Perp16.5		$i_{\perp} \approx 0.025 – 0.1$	≈ 0.01

Additionally, for the conditions of test *Par8.0* also a long duration test with a constant 'orbital' velocity yielding $i_{//} \approx 0.01$, was run for a one-week duration. One standard test with perpendicular load *Perp8.0* was performed with weight added to the sand, amounting to a superimposed pressure of 17.7 kN/m^2, or roughly 2 m of sand.

4. Results

In this section the results of the tests are described. First that an example of the gradients is given, and after that the resulting critical gradients are presented.

In Figure 8 snapshots of the time signal of the plunger motion and resulting (parallel) gradient are shown. It can be seen that the plunger signal exhibits periods with alternating constant velocity (sloping lines) and constant amplitude. The switch in velocity is made with a limited acceleration. This results in periods with constant gradient and filter velocity. As the plunger stroke is constant, but the velocity increases, the duration of the periods with constant /gradient velocity decreases.

In Figures 9 and 10 the final observed critical gradients are plotted. Note that the error bars indicate the gradients that were produced in the last test that did not show sand erosion, and the first test where sand motion was observed. The critical situation was estimated as the mean values of these two gradients.

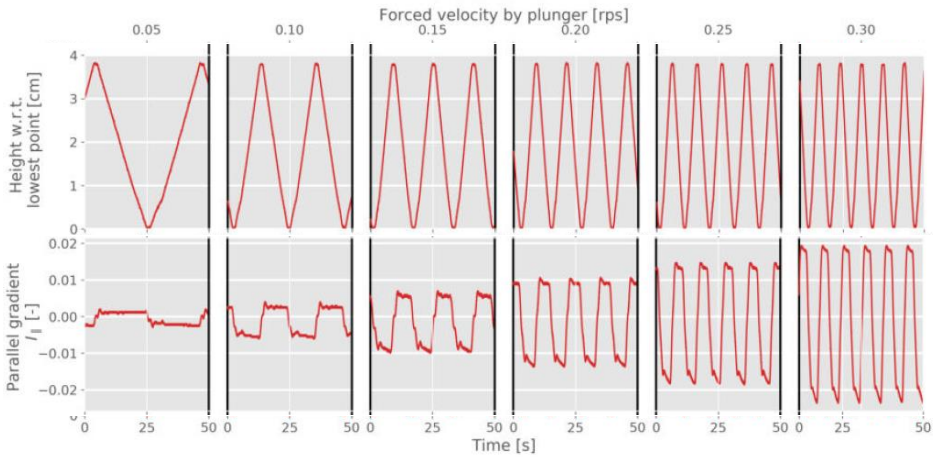

Figure 8. Samples of 50 s duration cut from test with different magnitudes of the stepwise increasing plunger velocity. Top: Measured parallel gradient. Bottom: measured piston motion.

The critical gradients for the parallel component are plotted in Figure 9. One test was done with a closed filter, with $D_{15F}/D_{85B} = 4$. As expected, no sand erosion could be observed here under the largest gradient that could be created of 8%. This point has been indicated in the figure by a upward triangle and arrow to indicate a lower boundary of the critical parallel gradient for the closed filter. In the range of $D_{15F}/D_{85B} = 7.5$ to 9.5 three filters were tested. Here critical parallel gradients of roughly 2% down to 1% were observed. Thus it seems that with respect to this gradient component the arching mechanism can yield some stability to a reversed filter. For the most open filter, characterized by $D_{15F}/D_{85B} = 16.5$, no stable gradient was found. The first gradient that was applied of about 0.25% already led to erosion.

For the perpendicular gradients similar results were found, as can be seen in Figure 10. The critical perpendicular gradients are about an order of magnitude larger than the critical parallel gradients. Critical gradients around $i_{\perp} \approx 0.1$ to 0.2 are observed for the somewhat open reversed filters. Again, for the very open filter no critical gradient is found.

For the long duration test with the just-below critical conditions obtained from Par8.0, no earlier erosion was observed. The tests with superimposed load was erroneously conducted with too large steps in plunger velocity. It could unfortunately not be seen whether the critical perpendicular load was increased or not.

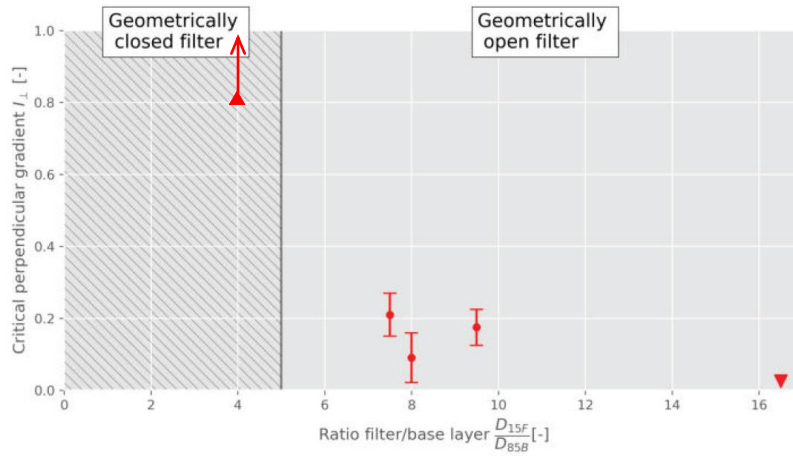

Figure 9. Critical perpendicular gradients as determined from the setup. Upward triangle: largest tested load without erosion. Downward triangle: lowest tested load with erosion.

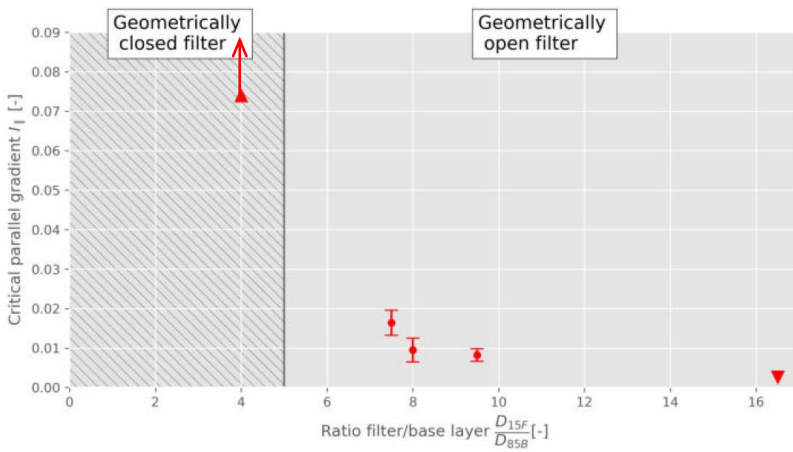

Figure 10. Critical parallel gradients as determined from the setup. Upward triangle: largest tested load without erosion. Downward triangle: lowest tested load with erosion.

5. Discussion

Perpendicular gradient during parallel gradient. In further tests after the presently reported study (Lengkeek 2022) it appeared that during the tests with parallel gradients, the lid might not be completely air/water tight. This potentially causes the presence of

perpendicular gradients during the tests that were intended to test on parallel gradients. These could actually be quite large and governing for the (in)stability of the tests. However, the actual parallel gradients were measured during the tests, so still serve as a lower, safe limit of the stability of the interface. New tests with a sealed lid, and simultaneous monitoring of the perpendicular gradient are advised (and planned).

Oblique waves. The current estimate for the occurring gradients has been made for wave attack normal to the coast. The effect of oblique wave attack needs to be considered. The perpendicular gradient is caused by the absolute pressure on the interface that drives the porous flow through the sand. As the travelling distance of the waves through the core of the bund increases for oblique wave attack, it is reasonable to expect the damping of the pressures to increase, such that the perpendicular gradient on the interface would decrease. Hence the assumption of normal wave attack is conservative for oblique cases. However, the parallel gradient is actually related to the flow through the porous core. This is reduced by the zero-velocity boundary condition at the sand interface. In case of oblique wave attack the wave motion inside the core material also has a shore-parallel component. This velocity component is not forced to zero at the boundary. So even though the pressure is damped further for oblique wave attack, the very low parallel gradient near the bed might even increase. This should be checked using physical, numerical or analytical models.

Sand in pores. The filter that was tested was completely cleaned between tests for efficiency reasons. However, during application of the sand on top of the granular filter, it could not be avoided that some loose sand penetrated into the gravel layer. Hence part of the observed sand motion in the tests might have originated from the pores, instead on the interface. This makes the results somewhat conservative, and safe to use.

Superimposed load. As can be seen in Figure 1, a large layer of sand is present above the lower parts of the gravel-sand interface that was studied. For normal filters, with sand on top of gravel, it was observed that particularly the critical perpendicular gradient increased by this imposed load (De Graauw et al. 1983). This was attributed to increased magnitude of the arching mechanism. Hence this effect could well be present for the reversed filter as well. Hence it should be quantified. In the present setup no conclusive results were obtained, but this warrants further study.

Installation of sand. The sand was installed on top of the gravel in a dry setup, before this was filled with water. However, in reality the installation will always be in the wet. This could alter the way that the sand ends up on the interface. In the setup it was observed it was difficult to place the sand on the gravel without it penetrating the filter. It might be that the sand will initially penetrate the filter and rock bund during installation as indicated in the figure below, a potentially more stable configuration. However, this infiltration of sand into the core seems nearly impossible to control or to inspect. Hence, it seems to be practical to still base the design of the filter on the present critical gradients.

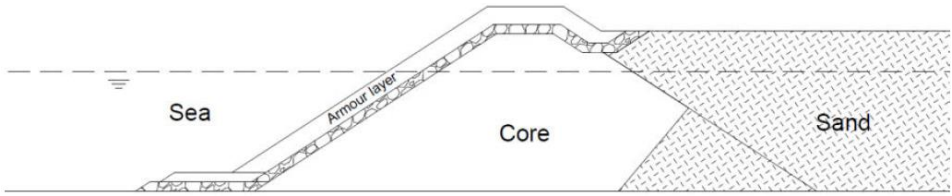

Figure 11. Rock bund with partial geotextile protection and sand penetrating the rock core (Tutein Noltenius, 2018).

Outflow from sand. It was seen that for internal setup flow into the sand core could occur. However, due to falling mean water levels also a steady flow out of the sand core could occur, which would influence the interface stability as well. This more stationary situation must also be taken into account.

Combined gradients. During wave action, also a combination of gradient components can be present at the interface. Simultaneously combined gradients can be simulated in the test setup, but it is not clear yet which combination will actually give representative gradient combinations.

Resemblance to real wave-induced gradients. The temporal shape of the simulated gradient was blocky, with periods of alternating constant gradient, as shown in Figure 8. The period decreases with increasing load, as the plunger stroke is constant. Because the aim was to detect initiation of motion, the main parameters that had to be mimicked where the magnitude of the gradient and the reversal of the direction. The duration should be comparable or larger than the period of maximum flow velocity on a sinusoidal wave motion. For the largest load the duration is still several seconds. Hence this effect is deemed to be negligible and at most slightly conservative for most real wave periods.

Towards practical application. The factors of influence discussed above need to be investigated before the method is deemed accurate. But we estimate the present results to be conservative. Hence, if the maximum gradients at an interface in a lifetime of a structure can be proven to be below the values determined in this study, for instance by a CFD model as shown in Figure 3, it is reasonable to deduce that the interface is stable with regards to the wave loads. Note that the CFD also has to be executed for oblique wave loads, which can still be computationally expensive. Analytical or empirical formulas for the load should be developed. Do note that besides wave loads, also other loads need to be considered, like stationary head differences and geotechnical, thermal and seismic influences.

5. Conclusions

In this paper the loads on a reversed open granular filter were studied. Such an open filter could be applicable for the lower parts of the interface between sand fill and a granular at a rock bund around a reclamation area.

A numerical model was used to estimate the hydraulic attack on the reversed open filter. The hydraulic gradients at the sand-gravel interface was simulated for a storm with H_s = 3.5 m, T_p = 12 s and h = 12.4 m. For this condition the perpendicular gradient at the sand-gravel interface $i_{//,2\%}$ was seen to be very low and tending towards zero near the bed (smaller than 0.1% for the lowest three meters). The perpendicular gradient $i_{\perp,2\%}$ was seen to have a finite magnitude around 0.25 near the bed, roughly similar to the incoming maximum wave amplitude divided by the layer of sand above it.

The strength of the reversed open filter was tested using a small plunger model setup with prototype materials and loads. The critical gradients were determined with oscillating velocities.

For D_{15F} / D_{85B} of 7.5 to 9.5, the critical parallel gradient was measured to be $i_{//,c} \geq 1\%$. The lowest part of the interface is expected to always be stable with regards to the parallel gradient, as $i_{//,2\%}$ it tends towards 0 near the bed. With regards to the perpendicular gradient the measured critical gradient was not clearly dependent on the filter-base ratio, D_{15F} / D_{85B}. It appears to be around 0.1 to 0.2, hence it is lower than the occurring loads for the case presently treated.

Due to the similar magnitude of occurring and critical parallel gradients, it seem plausible that for the lower parts of the filter layer for other cases, e.g. with a lower wave height or wider bund, the lower part of a reverse filter could be constructed as an open granular filter, with filter-base ratios of D_{15F} / D_{85B} of up to 10. A numerical CFD model like the OpenFOAM-VoF model used, seems a suitable design tool to determine the loads on the interface.

The results of this initial study are not conclusive, but promising. It seems possible that reversed open filters at lower parts of rock bunds covered with sand could be stable under wave loads under certain conditions. Somewhat more data on the exact critical loads would be required, especially on the influence of the potentially stabilizing superimposed load, oblique wave attack, falling water levels, and the simultaneous occurrence of the two gradient components.

References

Low, B.K., S.K. Tang, and V. Choa. *Arching in Piled Embankments*. Journal of Geortechnical Engineering, 120(11):1917–1938, 1995.

Chen, C.N., W.Y. Huang, and C.T. Tseng. (2011) *Stress Redistribution and Ground Arch Development During Tunneling. Tunnelling and Underground Space Technology* 26(1):228–235, 2011.

Chew, S.H., H. Tian, S.A Tan, and G.P. Karunaratne. (2003) *Erosion stability of punctured geotextile filters subjected to cyclic wave loadings — a laboratory study*. Geotextiles and Geomembranes, 21:221–239.

De Graauw, A., T. van der Meulen, and M. van der Does de Bye. (1983) *Design criteria for granular filters.* Technical Report January 1983, Delft Hydraulics (Deltares). 1983.

G. Enstad. *On the Theory of Arching in Mass Flow Hoppers*. Chemical Engineering Science, 30:1273–1283, 1975. ISSN 00092509. doi: 10.1016/0009-2509(75)85051-2.

Jacobsen, N.G., DR Fuhrman, J Fredsøe (2012) *A wave generation toolbox for the open - source CFD library: OpenFoam®* . International Journal for Numerical Methods in Fluids 70 (9), 1073-1088

Jacobsen, N.G., M.R.A. van Gent, G. Wolters (2015) *Numerical analysis of the interaction of irregular waves with two dimensional permeable coastal structures*. Coastal Engineering 102, 13-29

Lengkeek, R.A. (2022) *Geometrically Open Inverted Granular Filters*. Delft University of Technology. http://resolver.tudelft.nl/uuid:915628dc-cd8c-4362-8f9e-12ec7e3d52ff

Paik, K.H. and R. Salgado. *Estimation of Active Earth Pressure Against Rigid Retaining Walls Considering Arching Effects*. Geotechnique, 53(7):643–653, 2003. ISSN 00168505. doi: 10.1680/geot.2003.53.7.643.

Polidoro, A., W. Allsop, and T. Pullen. (2015) *Exploring the Need for Geotextile Filters for Rubble Bunds Retaining Sand-Fill Islands.* Proc. Coastal Structures and Solutions to Coastal Disasters 2015, pages 763–773, 2015.

Tutein Nolthenius, R. (2018) *Sandfill-Retaining rubble mound structures: Evaluating the behaviour of sediments at the interface of a rubble mound with a reclamation, by means of physical modelling*. MSc thesis. Delft University of Technology. http://resolver.tudelft.nl/uuid:8c255d44-f7b5-407f-ae2d-ddcc80eafe6d

Van de Ven, D.P. (2019) *Granular open filter in rubble mound sand retaining structures. Physical model tests of a negative geometrically open filter layer.* MSc thesis. Delft University of Technology.
http://resolver.tudelft.nl/uuid:4cf578d6-091f-4b72-9fa2-79c71c6398c3

Van Gent, M.R.A. (1995) *Porous Flow through Rubble-Mound Material.* Journal of Waterway Port Coastal and Ocean Engineering 121. ASCE.